

2D Numerical Model of Sediment Transport Under Dam-break Flow Using Finite Element

Qalbi Hafiyyan^{a,*}, Dhemi Harlan^b, Mohammad Bagus Adityawan^b, Dantje Kardana Natakusumah^c,
Ikha Magdalena^d

^a Water Resources Development Center, Institut Teknologi Bandung, Bandung, 40116, Indonesia

^b Water Resources Engineering and Management, Institut Teknologi Bandung, Bandung, 40116, Indonesia

^c Water Resources Engineering Research Group, Institut Teknologi Bandung, Bandung, 40116, Indonesia

^d Industrial and Financial Mathematics Research Group, Institut Teknologi Bandung, Bandung, 40116, Indonesia

Corresponding author: *qhafiyyan@gmail.com

Abstract— The potential hazard of dam construction is the possibility of dam failure. Dam failure will cause damage to property and the environment, as well as loss of human life. In addition, the dam-break flow also causes erosion and sediment transport which can affect the morphology of rivers around the dam. Dam-break flow analysis is needed to minimize the potential hazards of dam construction. Dam-break flow analysis can be done by performing numerical modeling. This study develops a numerical model using the Taylor Galerkin method. The Taylor Galerkin model is used in simulating the dam-break flow along with the sediment transport that occurs. Mathematically, this flow is generally expressed by the shallow water-Exner equations. The shallow water equations describe the movement of water, and the Exner equation describes the movement of sediment. The model will use the Galerkin method for spatial derivatives and the Taylor series approach for time derivatives in this study. A numerical filter by Hansen was also added to the model to overcome the instability of the model due to numerical oscillations. To determine the performance of the Taylor Galerkin model, simulation results were compared with experimental data and other numerical results from previous studies. The Taylor Galerkin model can simulate the dam-break flow with sediment movement over a movable bed well based on this study. Studies like this are needed to reduce the high risk of dam failure.

Keywords— Dam-break; movable bed; Hansen filter; Taylor Galerkin.

Manuscript received 15 Feb. 2021; revised 21 Mar. 2021; accepted 1 Jun. 2021. Date of publication 31 Dec. 2021.
IJASEIT is licensed under a Creative Commons Attribution-Share Alike 4.0 International License.



I. INTRODUCTION

Dam construction carries a large potential risk in the form of possible dam failure [1]. Dam failure is an event where the dam collapses and causes the dam cannot keep the water. These events could negatively impact the property in the downstream area of the dam and the environment around the dam [2]–[7]. The dam-break flow causes erosion and sediment movement along the flow path. The effects of erosion and sediment movement may be even more dangerous than the effects of flooding [8]. Thus, a study on the dam-break flow needs to be carried out to minimize the impact of dam failure.

One way to study this flow is to do numerical modeling. Numerical modeling will be more effective than laboratory experiments. Dam-break flow hydraulic modeling has been done a lot. The modeling is generally formulated using

shallow water equations (SWE). Several numerical methods can solve this equation. These schemes are finite-difference [9]–[12], finite element [13]–[16], and finite volume method [17]–[21]. Of all these methods, the finite difference method is the most frequently used. This is due to its simplicity. However, the finite difference method tends to be unstable in dealing with shock waves [22]. The finite element method (FEM) and the finite volume method (FVM) have better stability than the finite difference method (FDM). Another advantage of FEM is its flexibility in handling cases with complex geometries. Thus, the finite element method is suitable for dam-break flow modeling. This is because the model domains tend to be irregular or complex.

In this study, it is necessary to combine morphodynamic and hydrodynamic equations. Morphodynamic equations describe erosion and sediment movement, while hydrodynamic equations describe water flow. The morphodynamic equation used is the Exner equation. Several

researchers have used the SWE-Exner model to simulate the dam-break flow and the sediment transport that occurs. The majority of these researchers use the FVM to solve the SWE-Exner model [23]–[25]. Meanwhile, not many researchers have used the FEM to solve the SWE-Exner model.

In the present study, the Taylor Galerkin method was used as a numerical scheme. This method was first developed by Donea [26]. The Taylor Galerkin method has a very simple algorithmic structure [27]. Also, the method does not need the determination of free parameters to maximize its accuracy [26]. The Taylor Galerkin model has been used in Zandrato [22] to simulate 1D dam-break flow without erosion and sediment movement. It shows that the Taylor Galerkin model is capable of simulating 1D dam-break flow. Zandrato [22] also shows that the Taylor Galerkin model gives more accurate results than the finite-difference model. The Taylor Galerkin model also successfully simulated a 2D dam-break flow on a non-erodible bed [28]. In the present study, the Taylor Galerkin model was used to simulate the dam-break flow along with the sediment transport that occurs. To reduce numerical oscillations on the Taylor Galerkin model, a numerical filter by Hansen was applied. The filter has been used successfully in some previous studies [15], [28], [29]. This paper aims to report the performance of the Taylor Galerkin model in simulating the dam-break flow with sediment transport over a movable bed either in one-dimensional or two-dimensional. The results of the model will be compared with experimental laboratory data. Also, it is compared with other numerical results from previous studies.

II. MATERIAL AND METHOD

A. Governing Equation

The governing equation comes from coupling the Exner equation and shallow water equations (SWEs). The shallow water equation is used to simulate water flow, while the Exner equation simulates sediment transport. The vector form of the 2D SWE-Exner equation is as follows (by ignoring suspended load, wind effect, the Coriolis force, momentum due turbulence and viscosity):

$$\frac{\partial U}{\partial t} + \frac{\partial F_x}{\partial x} + \frac{\partial F_y}{\partial y} = S \quad (1)$$

Where:

$$U = \begin{pmatrix} h \\ hu \\ hv \\ z \end{pmatrix} \quad (2)$$

$$F_x = \begin{pmatrix} uh \\ uvh \\ u^2h + \frac{1}{2}gh^2 \\ \frac{1}{(1-p)}q_{s,x} \end{pmatrix} \quad (3)$$

$$F_y = \begin{pmatrix} vh \\ v^2h + \frac{1}{2}gh^2 \\ uvh \\ \frac{1}{(1-p)}q_{s,y} \end{pmatrix} \quad (4)$$

$$S = \begin{pmatrix} 0 \\ gh(So_x - Sf_x) \\ gh(So_y - Sf_y) \\ 0 \end{pmatrix} \quad (5)$$

With h is water depth, g is gravitational acceleration, z is bed level, p is bed porosity, u is the water velocity in the x -direction, v is the water velocity in the y -direction, So_x and So_y denotes bottom slopes, $q_{s,x}$ and $q_{s,y}$ are sediment discharge per unit width, Sf_x and Sf_y correspond to bottom frictions. The bottom frictions can be calculated according to Manning's formula:

$$Sf_x = \frac{n^2 u (u^2 + v^2)^{1/2}}{h^{4/3}} \quad (6)$$

$$Sf_y = \frac{n^2 v (u^2 + v^2)^{1/2}}{h^{4/3}} \quad (7)$$

With n correspond to Manning's coefficient.

The sediment transport equations used in this study are Meyer-Peter & Muller (MPM) and Grass formula. Grass proposes a formula for sediment transport discharge as follows:

$$q_{s,x} = Ag u^2 (u^2 + v^2) \quad (8)$$

$$q_{s,y} = Ag v^2 (u^2 + v^2) \quad (9)$$

The constant A_g has a value between 0 and 1. If the value is close to 1, it means that the model describes a strong interaction between water and sediment particles. The constant is obtained based on experimental data.

The MPM formula is a sediment discharge formula based on the median grain diameter (d_{50}). The formula is as follows:

$$q_{s,x} = 8 \sqrt{g(s-1)d_{50}^2} (\max(0, \tau_{*,x} - \tau_{*,c}))^{0.5} \quad (10)$$

$$q_{s,y} = 8 \sqrt{g(s-1)d_{50}^2} (\max(0, \tau_{*,y} - \tau_{*,c}))^{0.5} \quad (11)$$

Typically, the critical bed-shear stress ($\tau_{*,c}$) is 0.047, while the bed-shear stress ($\tau_{*,x}$, $\tau_{*,y}$) can be calculated by the following equation:

$$\tau_{*,x} = \frac{n^2 q_x \sqrt{q_x^2 + q_y^2}}{(s-1)d_{50}h^{7/3}} \quad (12)$$

$$\tau_{*,y} = \frac{n^2 q_y \sqrt{q_x^2 + q_y^2}}{(s-1)d_{50}h^{7/3}} \quad (13)$$

with s is a relative density of fluids, q_x and q_y are unit discharge components.

B. Taylor Galerkin Method

This study uses the Taylor Galerkin method to overcome the governing equations. Donea [26] obtained this method by combining the Taylor series approach and the Galerkin method. This study uses linear triangular elements to discrete computational domains. The time derivative of the 2D SWE-Exner equations is solved using a second-order Taylor series as follows:

$$U^{n+1} = U^n + \Delta t \left(\frac{\partial U}{\partial t} \right)^n + \frac{\Delta t^2}{2} \left(\frac{\partial^2 U}{\partial t^2} \right)^n \quad (14)$$

Rearranging equation (1), so the time derivative in terms of space derivative as below:

$$\frac{\partial U}{\partial t} = S - \frac{\partial F_i}{\partial x_i} \quad (15)$$

And

$$\frac{\partial^2 U}{\partial t^2} = \frac{\partial S}{\partial t} - \frac{\partial}{\partial x_i} \left(\frac{\partial F_i}{\partial t} \right) = \frac{\partial S}{\partial U} \frac{\partial U}{\partial t} - \frac{\partial}{\partial x_i} \left(\frac{\partial F_i}{\partial U} \frac{\partial U}{\partial t} \right) = G \frac{\partial U}{\partial t} - \frac{\partial}{\partial x_i} \left(A_i \frac{\partial U}{\partial t} \right) \quad (16)$$

By substituting equation (15) to (16), the following equation is obtained:

$$\frac{\partial^2 U}{\partial t^2} = G \left(S - \frac{\partial F_i}{\partial x_i} \right) - \frac{\partial}{\partial x_i} \left(A_i \left(S - \frac{\partial F_j}{\partial x_j} \right) \right) \quad (17)$$

Then the equation below is obtained by substituting equations (15) and (17) into equation (14).

$$U^{n+1} = U^n + \Delta t \left(S - \frac{\partial F_i}{\partial x_i} \right)^n + \frac{\Delta t^2}{2} \left(G \left(S - \frac{\partial F_i}{\partial x_i} \right) - \frac{\partial}{\partial x_i} \left(A_i \left(S - \frac{\partial F_j}{\partial x_j} \right) \right) \right)^n \quad (18)$$

For space derivatives, several approximation functions are used as below:

$$U = U^i N_i \quad F = F_j^i N_i \quad U = S^i N_i \quad (19)$$

with N_i refers to the piecewise linear shape function for node i .

$$G = G_j^e P_e \quad A = A_j^e P_e \quad (20)$$

where P_e corresponds to piecewise constant shape function for element e . The next step, equation (18) is then weighted with the shape functions N_i to obtain

$$\int_{\Omega} \Delta U N_i d\Omega = \Delta t \int_{\Omega} \left(S - \frac{\partial F_i}{\partial x_i} \right)^n N_i d\Omega + \frac{\Delta t^2}{2} \int_{\Omega} \left(G \left(S - \frac{\partial F_j}{\partial x_j} \right) - \frac{\partial}{\partial x_j} \left(A_j \left(S - \frac{\partial F_k}{\partial x_k} \right) \right) \right)^n N_i d\Omega \quad (21)$$

where Ω is the computational domain. Consistent mass matrix (M) is given by

$$M_{ij} = \int_{\Omega} N_i N_j d\Omega \quad (22)$$

Gauss Theorem is applied to equation (21) to obtain a weak form. After that, the two sides of the equation (21) are multiplied by N_j , and using the consistent mass matrix, the following equation will be obtained

$$M \Delta U = \Delta t \int_{\Omega} \left(S - \frac{\partial F_k}{\partial x_k} \right)^n N_i N_j d\Omega + \frac{\Delta t^2}{2} \left\{ \int_{\Omega} \left(G \left(S - \frac{\partial F_k}{\partial x_k} \right)^n N_i - \left(A_k \left(S - \frac{\partial F_l}{\partial x_l} \right) \right)^n \frac{\partial N_i}{\partial x_k} \right) N_j d\Omega - \int_{\Gamma} \left(A_k \left(S - \frac{\partial F_l}{\partial x_l} \right) \right)^n N_i N_j n_k d\Gamma \right\} \quad (23)$$

where n_k is a normal vector component to boundary Γ . Equation (23) can be solved with a two-step algorithm as in [30], then the final equation will be obtained as follows:

$$M \Delta U = \Delta t \left\{ \int_{\Omega} \left(\begin{array}{l} \left[S^{n+1/2} N_i + \left[S^{n+1/2} - \bar{S}^n \right] N_j + \right. \\ \left. \left[F_x^{n+1/2} N_i + \left[F_x^{n+1/2} - \bar{F}_x^n \right] \frac{\partial N_j}{\partial x} + \right. \right. \\ \left. \left. \left[F_y^{n+1/2} N_i + \left[F_y^{n+1/2} - \bar{F}_y^n \right] \frac{\partial N_j}{\partial y} \right] \right) \right) d\Omega + \int_{\Gamma} \left(\begin{array}{l} \left[-F_{xi} n_x N_i - \left[F_x^{n+1/2} - \bar{F}_x^n \right] n_x \right] N_j + \\ \left[-F_{yi} n_y N_i - \left[F_y^{n+1/2} - \bar{F}_y^n \right] n_y \right] N_j \end{array} \right) d\Gamma \right\} \quad (24)$$

C. Numerical Filter

In this study, the Taylor Galerkin model will be added with a numerical filter. Its purpose is to reduce numerical oscillations in the model and to obtain better stability. The numerical filter will be applied to each computational point in each iteration of time. Parameters such as bed level, the velocity of flow, and water depth will be updated using the equation below:

$$P_{i,j} = P_{i,j} \times C + \frac{P_{i+1,j} + P_{i-1,j} + P_{i,j+1} + P_{i,j-1}}{4} \times (1 - C) \quad (25)$$

The correction factor (C) used is 0.99, with P is according to the parameters filtered.

III. RESULT AND DISCUSSION

A. 1D Experimental Dam-break Over Erodible Bed

A case with experimental data is presented. This case was conducted in a rectangular flume at the UCLouvain [31]. The flume was 6 m long. Then, there is a gate located in the center of the flume simulating an idealized dam. The water depth at the upstream part is 0.35 m. Meanwhile, the downstream part is in dry conditions. The initial bed level is set to zero, and Manning's roughness coefficient is assumed 0.001. In this test case, the grass equation is used to calculate the sediment discharge with $Ag = 0.005$ and $P = 0.3$.

Fig. 1 represents the experimental and numerical results of the bed profile and water level for $t = 1$ second. A good agreement between the experimental results and the Taylor Galerkin solutions was found for the bed profile and water level. A good agreement is also seen between the Taylor Galerkin simulation results and the numerical results by Magdalena *et al.* [25].

B. 1D Hypothetical Dam-break Over Movable Bed

Magdalena *et al.* [25] have performed an analysis of this hypothetical case. The computational domain for the hypothetical case is 10 m x 1 m, divided by 8000 linear triangular elements. The position of the dam is in the center of the computational domain. In the beginning, the dam is assumed to break down instantaneously. The water body is assumed stationary. Initially, upstream water was 2 m high, and downstream water was 0.125 m high. Then, the initial bed level is set to zero. The bed is assumed to be frictionless. In

this case, the grass formula (with $A_g = 0.005$ and $P = 0.3$) is used to calculate the sediment transport.

Fig. 2 shows the bed profile and water level at time $t = 1$ second after dam failure, where the solid dots represent Taylor Galerkin model results, and the lines illustrate the numerical results of the previous study. From this figure, it can be seen that the flood waves are propagating downstream. The flood waves caused scouring around the dam site. Flood waves also cause an increase in bed elevation in the downstream area. This is due to the flood waves bringing along the scoured sediment particles. Fig. 2 also shows that the Taylor Galerkin model has also given a good comparison with the simulation results by Magdalena et al. [25].

To determine the model's performance developed, the model results will be compared with experimental data and numerical solutions from other studies. Comparison of the evolution of water levels between experimental and numerical results is presented in Fig. 4 and Fig. 5. From this figure, the Taylor Galerkin solutions show good trends concerning experimental data and other numerical solutions.

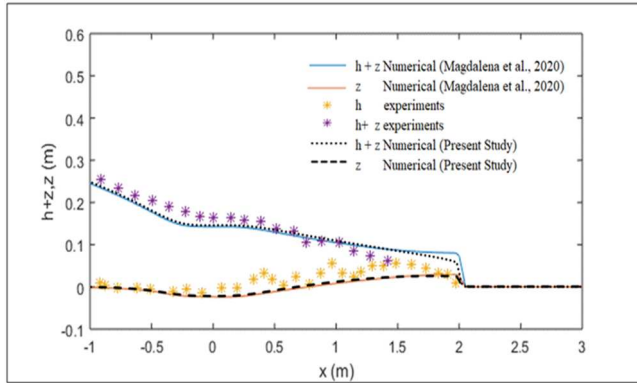


Fig. 1 Bed profile and water level ($t = 1$ s) for 1D experimental case

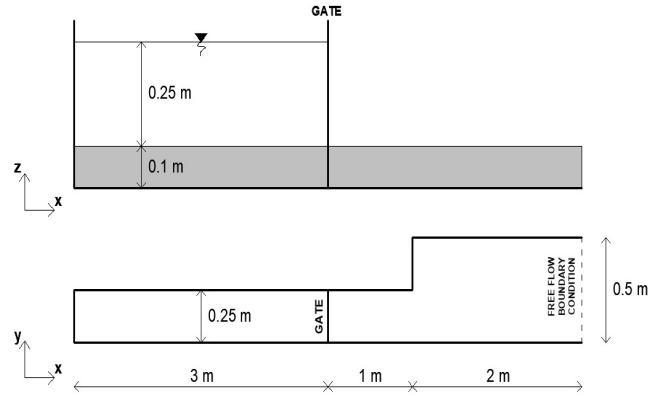


Fig. 3 Sketch the initial conditions

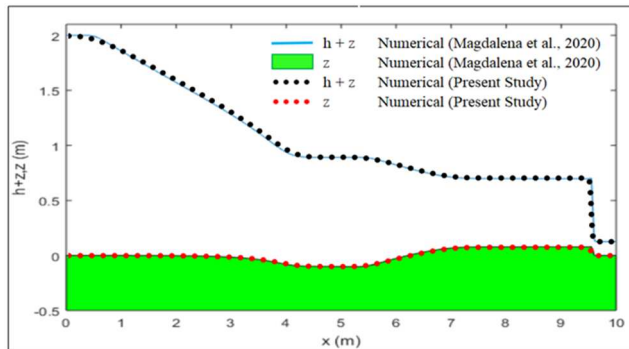


Fig. 2 Comparison of the simulation results ($t = 1$ s) for the hypothetical case

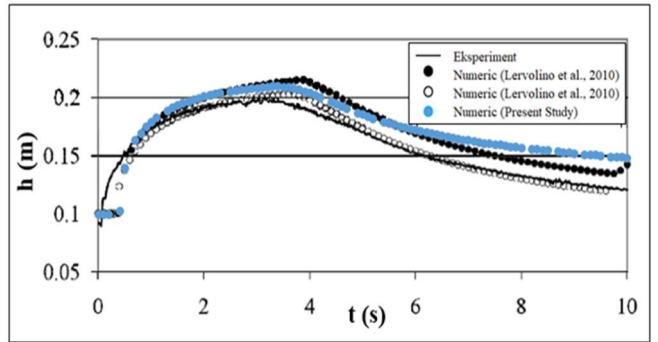


Fig. 4 Water surface at P1

C. 2D Dam-break Flow on Erodible Bed in Sudden Expansion Channel

Lervolino *et al.* [32] have analyzed the case of 2D dam-break flow on an erodible bed in a sudden expansion channel. This experiment was carried out on a flume. The width of the flume has expanded from 25 cm to 50 cm. The expansion occurs at a distance of 1 m to the right of the gate (see Fig. 3). Meanwhile, the length of the flume is 6 m. The bed material was uniform sand coarse. The specific density was 2.63, and the median grain diameter was 1.72 mm and. Initially, the bottom of the flume consisted of a layer of sand 0.100 m thick. The sand layer is fully saturated and compacted. Upstream, there is a layer of clear water as high as 0.25 m (see Fig. 3). The initial state of water at rest and the outlet is assumed to be free flow. In this test case, we assume that the coefficient of Manning is 0.025. The water level fluctuation is measured at two different points. The first point located at $x = 3.75$ m and $y = 0.125$ m is called P1. In comparison, the second point is at $x = 4.2$ m and $y = 0.125$ m which is called P2.

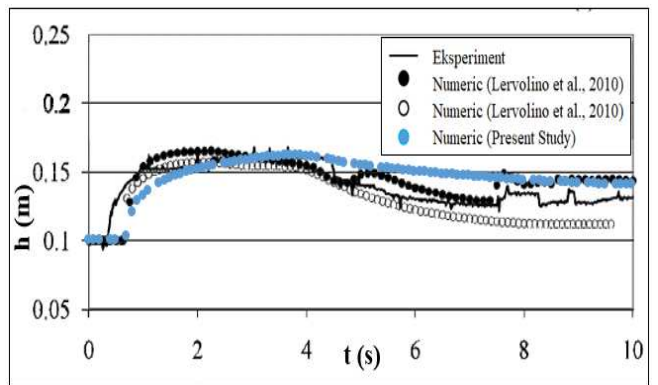


Fig. 5 Water surface at P2

Fig. 6 represents the contour changes of the bed level over time. From Fig. 6, it can be seen that the sediment particles are moved downstream. The bed level after the gate has increased over time. This is due to the supply of sediment particles from the upstream direction.

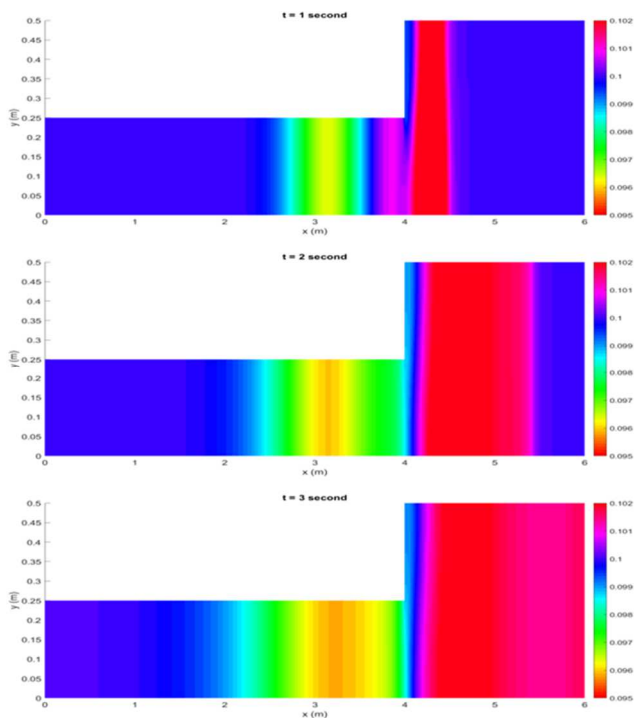


Fig. 6 Contour of bed level at different time

IV. CONCLUSION

This study developed the Taylor Galerkin scheme to solve the 2D SWE-Exner equations for computing dam-break flow with sediment movement over a movable bed. The scheme uses the Taylor series approximation for time derivatives and the Galerkin method for spatial derivatives. The Hansen filter is applied to reduce oscillation due to numerical instability in the model. Then, the performance of the developed model is tested for some dam-break cases. Based on the numerical results, Taylor Galerkin numerical scheme with the Hansen filter succeeded in simulating the dam-break problem over a movable bed.

ACKNOWLEDGMENT

P3MI LPPM ITB supports this research.

REFERENCES

- [1] H. Qian, Z. Cao, H. Liu, and G. Pender, "New experimental dataset for partial dam-break floods over mobile beds," *J. Hydraul. Res.*, vol. 56, no. 1, pp. 124–135, 2018, doi: 10.1080/00221686.2017.1289264.
- [2] V. Hatje *et al.*, "The environmental impacts of one of the largest tailing dam failures worldwide," *Sci. Rep.*, vol. 7, no. 1, pp. 1–13, 2017, doi: 10.1038/s41598-017-11143-x.
- [3] F. F. do Carmo *et al.*, "Fundão tailings dam failures: the environment tragedy of the largest technological disaster of Brazilian mining in global context," *Perspect. Ecol. Conserv.*, vol. 15, no. 3, pp. 145–151, 2017, doi: 10.1016/j.pecon.2017.06.002.
- [4] L. H. Silva Rotta *et al.*, "The 2019 Brumadinho tailings dam collapse: Possible cause and impacts of the worst human and environmental disaster in Brazil," *Int. J. Appl. Earth Obs. Geoinf.*, vol. 90, no. January, p. 102119, 2020, doi: 10.1016/j.jag.2020.102119.
- [5] V. E. Glotov, J. Chlachula, L. P. Glotova, and E. Little, "Causes and environmental impact of the gold-tailings dam failure at Karamken, the Russian Far East," *Eng. Geol.*, vol. 245, pp. 236–247, 2018, doi: 10.1016/j.enggeo.2018.08.012.
- [6] C. dos Santos Vergilio *et al.*, "Immediate and long-term impacts of one of the worst mining tailing dam failure worldwide (Bento Rodrigues, Minas Gerais, Brazil)," *Sci. Total Environ.*, vol. 756, p. 143697, 2021, doi: 10.1016/j.scitotenv.2020.143697.

- [7] K. T. O. Coimbra, E. Alcântara, and C. R. de Souza Filho, "An assessment of natural and manmade hazard effects on the underwater light field of the Doce River continental shelf," *Sci. Total Environ.*, vol. 685, pp. 1087–1096, 2019, doi: 10.1016/j.scitotenv.2019.06.127.
- [8] B. Spinewine and Y. Zech, "Small-scale laboratory dam-break waves on movable beds," *J. Hydraul. Res.*, vol. 45, no. SPEC. ISS., pp. 73–86, 2007, doi: 10.1080/00221686.2007.9521834.
- [9] X. Li, G. Li, and Y. Ge, "A new fifth-order finite difference weno scheme for dam-break simulations," *Adv. Appl. Math. Mech.*, vol. 13, no. 1, pp. 58–82, 2020, doi: 10.4208/AAMM.OA-2019-0155.
- [10] P. W. Li and C. M. Fan, "Generalized finite difference method for two-dimensional shallow water equations," *Eng. Anal. Bound. Elem.*, vol. 80, pp. 58–71, 2017, doi: 10.1016/j.enganbound.2017.03.012.
- [11] Z. Wang, J. Zhu, and N. Zhao, "A new fifth-order finite difference well-balanced multi-resolution WENO scheme for solving shallow water," *Comput. Math. with Appl.*, vol. 80, no. 5, pp. 1380–1387, 2020, doi: 10.1016/j.camwa.2020.07.003.
- [12] H. M. Kalita, "A simple and efficient numerical model for simulating one dimensional dam break flows," *Int. J. Hydrol. Sci. Technol.*, vol. 10, no. 1, pp. 1–16, 2020, doi: 10.1504/IJHST.2020.104985.
- [13] H. Lee, "Implicit discontinuous Galerkin scheme for shallow water equations," *J. Mech. Sci. Technol.*, vol. 33, no. 7, pp. 3301–3310, 2019, doi: 10.1007/s12206-019-0625-2.
- [14] O. Seydashraf and A. A. Akhtari, "Two-dimensional numerical modeling of dam-break flow using a new TVD finite-element scheme," *J. Brazilian Soc. Mech. Sci. Eng.*, vol. 39, no. 11, pp. 4393–4401, 2017, doi: 10.1007/s40430-017-0776-y.
- [15] D. Harlan, M. B. Adityawan, D. K. Natakusumah, and N. L. H. Zentrato, "Application of numerical filter to a Taylor Galerkin finite element model for movable bed dam break flows," *Int. J. GEOMATE*, vol. 16, no. 57, pp. 209–216, 2019, doi: 10.21660/2019.57.70809.
- [16] G. Li, L. Song, and J. Gao, "High order well-balanced discontinuous Galerkin methods based on hydrostatic reconstruction for shallow water equations," *J. Comput. Appl. Math.*, vol. 340, pp. 546–560, 2018, doi: 10.1016/j.cam.2017.10.027.
- [17] O. Castro-Orgaz and H. Chanson, "Ritter's dry-bed dam-break flows: positive and negative wave dynamics," *Environ. Fluid Mech.*, vol. 17, no. 4, pp. 665–694, 2017, doi: 10.1007/s10652-017-9512-5.
- [18] J. Fernández-Pato, M. Morales-Hernández, and P. García-Navarro, "Implicit finite volume simulation of 2D shallow water flows in flexible meshes," *Comput. Methods Appl. Mech. Eng.*, vol. 328, pp. 1–25, 2018, doi: 10.1016/j.cma.2017.08.050.
- [19] C. Di Cristo, M. Greco, M. Iervolino, R. Martino, and A. Vacca, "A remark on finite volume methods for 2D shallow water equations over irregular bottom topography," *J. Hydraul. Res.*, vol. 59, no. 2, pp. 337–344, 2020, doi: 10.1080/00221686.2020.1744752.
- [20] I. Kissami, M. Seaid, and F. Benkhalidoun, "Numerical assessment of criteria for mesh adaptation in the finite volume solution of shallow water equations," *Adv. Appl. Math. Mech.*, vol. 12, no. 2, pp. 503–526, 2020, doi: 10.4208/AAMM.OA-2019-0011.
- [21] Y. Lakhlifi, S. Daoudi, and F. Boushaba, "Dam-Break computations by a dynamical adaptive finite volume method," *J. Appl. Fluid Mech.*, vol. 11, no. 6, pp. 1543–1556, 2018, doi: 10.29252/jafm.11.06.28564.
- [22] N. Lely Hardianti Zentrato, D. Harlan, M. Bagus Adityawan, and D. Kardana Natakusumah, "1D Numerical modelling of dam break using finite element method," *MATEC Web Conf.*, vol. 270, p. 04022, 2019, doi: 10.1051/mateconf/201927004022.
- [23] R. Meurice and S. Soares-Frazão, "A 2D HLL-based weakly coupled model for transient flows on mobile beds," *J. Hydroinformatics*, vol. 22, no. 5, pp. 1351–1369, 2020, doi: 10.2166/hydro.2020.033.
- [24] A. Hosseinzadeh-Tabrizi and M. Ghaeini-Hessaroeiyeh, "Modelling of dam failure-induced flows over movable beds considering turbulence effects," *Comput. Fluids*, vol. 161, pp. 199–210, 2018, doi: 10.1016/j.compfluid.2017.11.008.
- [25] I. Magdalena, M. B. Adityawan, and C. Jonathan, "Numerical model for dam break over a movable bed using finite volume method," *Int. J. GEOMATE*, vol. 19, no. 71, pp. 98–105, 2020, doi: 10.21660/2020.71.27074.
- [26] J. Donea, "A Taylor-Galerkin method for convective transport problems," *Int. J. Numer. Methods Eng.*, vol. 20, no. 1, pp. 101–119, 1984, doi: 10.1002/nme.1620200108.
- [27] C. B. Jiang, M. Kawahara, and K. Kashiwama, "A Taylor-Galerkin-based finite element method for turbulent flows," *Fluid Dyn. Res.*, vol. 9, no. 4, pp. 165–178, 1992, doi: 10.1016/0169-5983(92)90003-F.
- [28] Q. Hafiyyan, M. B. Adityawan, D. Harlan, D. K. Natakusumah, and I. Magdalena, "Comparison of Taylor Galerkin and FTCS models for

- dam-break simulation,” *IOP Conf. Ser. Earth Environ. Sci.*, vol. 737, no. 1, 2021, doi: 10.1088/1755-1315/737/1/012050.
- [29] M. B. Adityawan and H. Tanaka, “Bed stress assessment under solitary wave run-up,” *Earth, Planets Sp.*, vol. 64, no. 10, pp. 945–954, 2012, doi: 10.5047/eps.2011.02.012.
- [30] Q. Hafiyyan, “Two Dimensional Modelling of Dam-break Flow Over Movable Bed Using Taylor Galerkin Finite Element Method,” Bandung Institute of Technology (ITB), Bandung, 2020.
- [31] B. Spinewine and H. Capart, “Intense bed-load due to a sudden dam-break,” *J. Fluid Mech.*, vol. 731, pp. 579–614, 2013, doi: 10.1017/jfm.2013.227.
- [32] M. Iervolino, A. Leopardi, S. Soares-Frazão, C. Swartenbroeckx, and Y. Zech, “2D-H Numerical Simulation of Dam-Break Flow on Mobile Bed with Sudden Enlargement,” *River Flow 2010*, 2010.